Supporting Information

Carrasco et al. 10.1073/pnas.1303035110

SI Materials and Methods

DNA Substrates. DNA substrates were produced by PCR from a series of related plasmid construct templates. These templates are based on the parent plasmid pSP73-JY0 (1, 2) with a variety of modifications as detailed below. The parent plasmid consists of the cloning vector pSP73 (~2.5 kbp) with a 5.3-kbp insert between the XhoI and BamHI sites consisting of a Crossover hotspot instigator (Chi)-free DNA region of *Escherichia coli* genomic DNA (*E. coli* K12 W3110 genome between positions 2,104,007 and 2,109,277 with the single natural Chi sequence removed). The cloning vector portion of the plasmid contains several Chi sequences, many of which are not easily removed as they occur in the β-lactamase coding region of the plasmid. Standard substrates contain five single Chi sequences appropriately oriented for recognition and are positioned 509, 1,450, 1,695, 1,835, and 2,152 bp from the distal DNA end. For substrates with an "Inverted" orientation (Chi3-For-Inverted) these single Chi sequences occupy the proximal region of the substrate DNA. Six of them are appropriately oriented for recognition and are positioned 37, 76, 297, 792, 1,437, and 2,098 bp from the AddAB entry point. To make the plasmids with multiple Chi sequences at defined positions, additional short inserts containing 3 or 10 closely spaced Chi sequences, which we refer to as Chi loci, were subsequently inserted into the Chi-free region of pSP73-JY0 (at the NheI and/or XbaI sites) in either orientation. The DNA sequences of these Chi loci are shown in Table S2 with *Bacillus subtilis* Chi sequences (5′-AGCGG) underlined. Note that the Chi sequence is recognized only by AddAB enzymes approaching from the 3′ side of this sequence as written.

Substrates for the magnetic tweezers experiments were generated by PCR, using a high-fidelity DNA polymerase (Phusion Polymerase; NEB), one digoxigenin (DIG)-labeled primer (distal end), and one unlabeled primer (proximal end) (Table S3). PCR conditions were as described by the manufacturer and products were checked by gel electrophoresis. To minimize DNA damage in our substrates, they were not exposed to intercalant dyes or UV radiation during their production and were stored at 4 °C for less than 1 mo.

Biotinylated AddAB. Experiments were performed with AddAB complexes containing a single biotin moiety at the N terminus of the AddA subunit. The wild-type biotinylated complex was produced as described previously for a nuclease-deficient mutant AddAB complex (1). We also generated a variant wild-type complex with a longer polyglycine linker (seven instead of the standard three glycines) between the biotin tag peptide sequence and the AddB subunit. The resulting complex behaved identically to the three-glycine linker complex used in the experiments presented in the main text. The biotinylated mutant complex $AddAB^{F210A}$ was produced by subcloning the mutant *addB* gene from vectors used in previous work (3) into vectors appropriate for coexpression with biotinylated AddA that were equivalent to those used for the wild-type AddAB complex. The mutant complexes were expressed and purified in the same manner as the wild-type enzyme.

Bulk Translocation Assay. Triplex displacement assays were modified from published methods (4, 5). Briefly, the pBR322 plasmid was engineered at an EcoRI site to contain a unique triplex binding site 2,065 bp away from the NdeI site. The NdeI-linearized plasmid was purified and annealed to 5′-carboxytetramethylrhodamine (TAMRA)-labeled triplex-forming oligonucleotide (TFO) according to published methods (4). Free TAMRA-TFO was removed using S400 spin columns (GE Healthcare). Assays were performed at the temperature indicated, using an SF61-DX2 stopped-flow fluorimeter with a mercury-xenon lamp (TgK Scientific Limited). The excitation light was set at 547 nm with a 570-nm cutoff filter placed between the sample and the photomultiplier tube. All of the concentrations stated are for the final samples after mixing in the stopped-flow apparatus. The reaction buffer contained 25 mM Tris acetate (pH 7.5), 2 mM magnesium acetate, 1 mM DTT, and 100 $\mu g \cdot mL^{-1}$ BSA. DNA substrates (1-nM molecules) were incubated in reaction buffer for 5 min with AddAB enzyme (5 nM) to preform AddAB–DNA complexes. Reactions were initiated by rapidly mixing the AddAB–DNA complex against 1 mM ATP.

Steady-State ATPase Assay. Two oligonucleotides (Eurofins MWG Operon) that were both devoid of Chi sequences and contained the sequences 5′-TTT TTT TTT TTT TTT TTT TTT TTT TTA TCT TGC GAG TCT TGC GAG TAT GCG AGT GTT GCG AGT TCG CGA GAT T-3′ and 5′-AAT CTC GCG AAC TCG CAA CAC TCG CAT ACT CGC AAG ACT CGC AAG ATA-3′ were annealed by heating to 95 °C for 5 min and slow cooling to room temperature over a period of 4 h. This yielded a partial duplex DNA substrate containing a 25-nt poly(dT) 5′ overhang flanking a 48-bp duplex. ATPase assays were conducted in a lambda 35 UV/Vis Spectrophotometer (Perkin-Elmer), using a pyruvate kinase/lactate dehydrogenase (PK/LDH) coupled assay. AddAB enzyme (8 nM) was preincubated with DNA substrate (40 nM) for 2 min in a buffer containing 25 mM Tris-acetate (pH 7.5), 2 mM magnesium acetate, 1 mM DTT, 40 $units \cdot mL^{-1}$ pyruvate kinase (Sigma), 40 $units \cdot mL^{-1}$ lactate dehydrogenase (Sigma), 1.5 mM phosphoenolpyruvic acid (Sigma), and 100 $\mu g \cdot mL^{-1}$ NADH (Sigma) at 22 °C. Reactions were initiated by the addition of ATP to 1 mM and the absorbance at 340 nm was subsequently monitored. Initial ATP hydrolysis rates were calculated by linear regression of the ATPase data (GraphPad Prism) and using the extinction coefficient of 6,200 $M^{-1} \cdot cm^{-1}$ for NADH.

Pre-Steady-State ATPase Assay. DNA substrates (600 bp) were made by PCR, using one biotinylated primer (ATDbio) and Phusion DNA polymerase (NEB). PCR products were purified after electrophoresis through 1% agarose gels run in 1× TAE buffer, using a gene jet gel extraction kit (Thermo). DNA was dialyzed overnight against a buffer containing Tris·Cl (10 mM) and EDTA (0.1 mM). DNA substrates (2 nM) were incubated with streptavidin (20 nM; Sigma) in a buffer containing BSA (100 $\mu g \cdot mL^{-1}$; Sigma), Tris-acetate (25 mM, pH 7.5), magnesium acetate (2 mM), DTT (1 mM), and a phosphate mop system consisting of 7-methylguanosine (200 μM; Sigma) and 0.01 $unit \cdot \mu L^{-1}$ bacterial PNPase (Sigma). This solution was left at room temperature for 30 min to allow efficient phosphate removal by PNPase before placing it on ice. The phosphate mop is not significantly active on the timescale (~5 s) of the experiments. AddAB enzyme (20 nM) and the phosphate sensor MDCC-PBP (N-[2-(1-maleimidyl)ethyl]-7-(diethylamino)coumarin-3-carboxamide phosphate binding protein) [5 μM, gift from Martin Webb (6)] were added to DNA mixes and incubated at 22 °C for 2 min before mixing against an equal volume of a solution containing heparin (1 $mg \cdot mL^{-1}$), ATP (1 mM), BSA (100 $\mu g \cdot mL^{-1}$; Sigma), Tris-acetate (25 mM, pH 7.5), magnesium acetate (2 mM), DTT (1 mM), 7-Methylguanosine (200 mM; Sigma), 0.01 $unit \cdot \mu L^{-1}$ bacterial PNPase (Sigma), and MDCC-PBP (5 μM). This solution was also preincubated at room

temperature for 30 min before MDCC-PBP addition. MDCC-PBP was excited at 436 nm with slit widths of 1.8 nm and the resulting fluorescence was recorded with a >455-nm cut-on filter at 22 °C. The change in fluorescence associated with phosphate production was calibrated using a phosphate standard solution (Sigma) in reaction buffer and heparin but in the absence of PNPase and AddAB.

Bulk Chi Recognition Assay. A 5,399-bp DNA substrate (1 nM) containing a locus of 10 Chi sequences 1,210 bp from one DNA end was incubated in a buffer containing Tris-acetate (25 mM), magnesium acetate (2 mM), DTT (1 mM), single stranded binding protein (2 μM tetramer), and ATP (1 mM) at 37 °C or 20 °C for 2 min. AddAB enzymes were added to the concentration indicated in Fig. S2 and the reaction was allowed to proceed for 1 min. An equal volume of stop solution containing Proteinase K (NEB) (1 mg·mL^{-1}), EDTA (100 mM), Ficoll 400 [10% (wt/vol)], SDS [5% (wt/vol)], Bromophenol blue (0.125%), and Xylene Cyanol (0.125%) was added and the sample was incubated at 20 °C for 10 min before loading onto a 1% TAE gel that was run at 30 V for 18 h. Gels were dried and exposed to a phosphor screen and imaged using a Typhoon 9400 phosphorimager (Molecular Dynamics). Chi fragment yield as a percentage of substrate DNA depleted was quantified as described previously (3).

Correlation Between Chi-Like Sequences and Pauses Histograms. Normalized histograms of Chi-like sequences and pauses occurrences were subjected to several correlation algorithms implemented in OriginLab. These provide a value between −1 and 1 that reflects the strength of the relationship between two random variables. Positive value means a positive correlation between the two variables. We computed three correlation coefficients: the Pearson product moment correlation coefficient, the Spearman rank correlation coefficient, and the Kendall correlation coefficient. We found a positive correlation between the experimental pause distribution data and the theoretical calculation of Chi-like sequences distribution, using the three correlation algorithms (Fig. S5). Correlations between Chi3-For and Chi3-For-Inverted showed poor values or even anticorrelation.

Relative Mean Velocity Curve in Single-Molecule Experiments. For comparison of relative rates as a function of DNA position (Figs. 2*C*, 3*C*, 3*F*, 5*C*, and 5*E* and Fig. S3*B*) individual instantaneous velocity traces were normalized by their mean velocities and averaged. Averaging caused some broadening of the downward spikes characteristic from pausing but without applying this procedure, changes in velocity are misrepresented because too much weight is given to velocity changes in "fast" AddAB enzymes and vice versa. To present a meaningful translocation value to the reader, the dimensionless relative mean velocity was multiplied by the overall mean velocity of all traces, which was 275 bp·s^{-1}.

Pauses Determination in Single-Molecule Experiments. In DNA replication traces, Ibarra et al. classified pauses as velocity points below a threshold given by 2 SD of the velocity distribution for moving enzymes (7). However, their experiments were performed at much larger forces, minimizing thermal contributions to the movement of the bead. Because our data were obtained at low force (3 pN vs. 23 pN), our distributions were three times wider. Moreover, the large variability of velocities observed within an AddAB translocation run due to dynamic disorder often made the velocity distribution overlap with that measured at no ATP. Therefore, we decided to instead use the velocity distribution at no ATP, which was always narrower, as representative of the pause state and take 3 SD as the pause threshold. Nevertheless, some of the traces were analyzed using the method described in Ibarra et al. (7) and this provided a similar pause duration and localization to the results presented in the main text. Our semiautomated approach to detect pauses disregards potential pause events that occurred in a shorter timescale than the resolution of the assay (0.35 s).

Pause Length Distributions. Pause durations were plotted as histograms with a bin size of 0.35 s. Distributions were then normalized by the total area and fitted to a normalized gamma function $y_{norm}(t) = \frac{k^N}{\Gamma(N)} t^{N-1} e^{-kt}$ with $\Gamma(N) = \int_0^\infty t^{N-1} e^{-t} dt$. Fits gave values for N and k that are represented in Table S1. Fits of non-normalized distributions to $y(t) = At^{N-1} e^{-kt}$ provided also very similar values for N and k. Errors in N and k were estimated as the SE of the fit.

1. Fili N, et al. (2010) Visualizing helicases unwinding DNA at the single molecule level. *Nucleic Acids Res* 38(13):4448–4457.
2. Yeeles JT, Dillingham MS (2010) The processing of double-stranded DNA breaks for recombinational repair by helicase-nuclease complexes. *DNA Repair (Amst)* 9(3):276–285.
3. Saikrishnan K, et al. (2012) Insights into Chi recognition from the structure of an AddAB-type helicase-nuclease complex. *EMBO J* 31(6):1568–1578.
4. Firman K, Szczelkun MD (2000) Measuring motion on DNA by the type I restriction endonuclease EcoR124I using triplex displacement. *EMBO J* 19(9):2094–2102.
5. McClelland SE, Dryden DT, Szczelkun MD (2005) Continuous assays for DNA translocation using fluorescent triplex dissociation: Application to type I restriction endonucleases. *J Mol Biol* 348(4):895–915.
6. Brune M, Hunter JL, Corrie JE, Webb MR (1994) Direct, real-time measurement of rapid inorganic phosphate release using a novel fluorescent probe and its application to actomyosin subfragment 1 ATPase. *Biochemistry* 33(27):8262–8271.
7. Ibarra B, et al. (2009) Proofreading dynamics of a processive DNA polymerase. *EMBO J* 28(18):2794–2802.

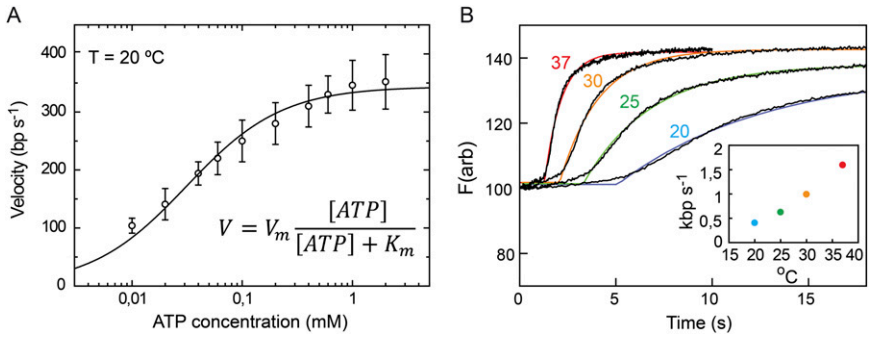

Fig. S1. AddAB velocity dependence on temperature and ATP concentration. (*A*) The relationship between translocation rate and ATP concentration in magnetic tweezers experiments. Experiments were performed on the Chi0 substrate at 3 pN force and at 20 °C. Pause-free velocities changed with ATP concentration in accordance with Michaelis–Menten kinetics, yielding a maximum velocity of $V_{max} = 344 \pm 7$ bp·s^{-1} and $K_m = 31 \pm 3$ μM. Errors are the SEM. (*B*) Bulk DNA translocation assays performed using the triplex displacement technique (1) (details in *SI Materials and Methods*). The substrate consisted of linearized plasmid DNA (1 nM) with an annealed TAMRA-labeled triplex positioned 2,065 bp away from the nearest free end. Triplex displacement curves were obtained by mixing a preformed AddAB–DNA complex with ATP (1 mM) in a stopped flow device at the temperature indicated and then monitoring the change in fluorescence as the triplex-forming oligonucleotide is displaced by the translocating enzyme. The data were fitted to an offset exponential to yield a lag time before triplex displacement. The distance traveled divided by the lag time yields an apparent translocation rate, and this is plotted as a function of temperature in the *Inset*. The values obtained at 37 °C are in good agreement with similar measurements made on different substrate DNA molecules (2). The translocation rate obtained at 20 °C is in good agreement with the net translocation rate obtained in the single-molecule experiments that are the main focus of this article.

1. Firman K, Szczelkun MD (2000) Measuring motion on DNA by the type I restriction endonuclease EcoR124I using triplex displacement. *EMBO J* 19(9):2094–2102.
2. Yeeles JT, van Aelst K, Dillingham MS, Moreno-Herrero F (2011) Recombination hotspots and single-stranded DNA binding proteins couple DNA translocation to DNA unwinding by the AddAB helicase-nuclease. *Mol Cell* 42(6):806–816.

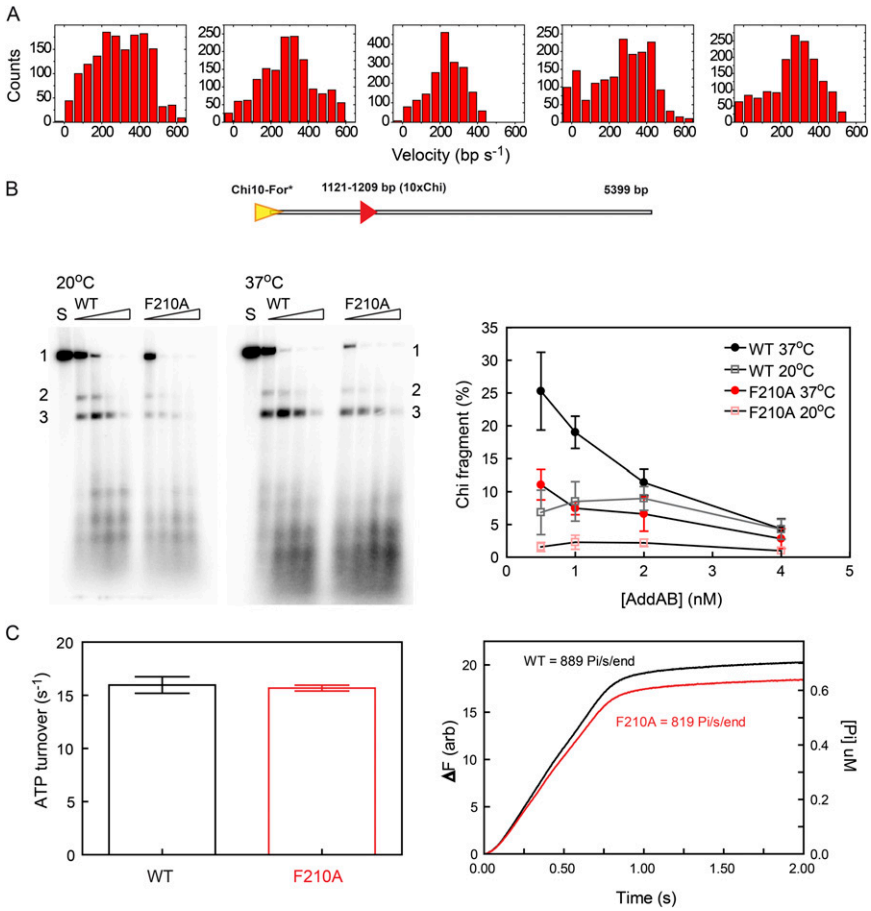

Fig. S2. Single-molecule static disorder, bulk ATPase, and Chi recognition efficiency. (*A*) Instantaneous velocity histograms of five independent time traces showing large variability of velocity distributions or static disorder. (*B*) Chi recognition assays in which 5′-radiolabeled DNA molecules (1 nM) containing a single 10×Chi locus were processed by AddAB or AddAB^{F210A} at the temperature indicated as described in *SI Materials and Methods*. The AddAB concentrations used in the experiment were 0.5, 1, 2, and 4 nM. The lane marked S is a control with unprocessed substrate DNA. The products of the reaction were separated on an agarose gel and the yield of the Chi fragment as a percentage of the total DNA processed (i.e., the substrate depleted) was calculated. Note that the Chi locus can be recognized only by AddAB enzymes approaching from the left DNA end as shown, and so the Chi fragment yield is, at best, equivalent to approximately one-half of the Chi recognition efficiency. For DNA molecules processed by two AddAB enzymes bound to each end of the substrate the Chi fragment is degraded by the AddAB enzyme approaching from the right end, and this explains the decreased apparent efficiency of recognition at high [AddAB]. Note that the substrate used (Chi10-For*) is almost identical to the Chi10-For except for the last section containing the parental cloning vector. (*C*) (*Left*) Steady-state ATPase activity of wild-type (WT) AddAB compared with the AddAB^{F210A} mutant measured using a PK/LDH coupled assay. Experiments were performed at 22 °C and 1 mM (saturating) ATP, using 8 nM AddAB and 40 nM oligoduplex DNA (Chi-free) in a reaction buffer containing 25 mM Tris-acetate (pH 7.5), 2 mM magnesium acetate, 1 mM DTT. (*Right*) Single-turnover phosphate release assay monitoring ATPase activity accompanying translocation on DNA measured using MDCC-PBP, a protein-based fluorescent probe for phosphate. Experiments were performed at 22 °C, using a preformed complex of 10 nM AddAB and 1 nM Chi-free DNA substrate in a reaction buffer containing 25 mM Tris-acetate (pH 7.5), 2 mM magnesium acetate, 1 mM DTT, and 0.1 mg/mL BSA. A heparin trap was added with the ATP, to eliminate ATP hydrolysis after the first interaction of the enzyme with the substrate. The DNA substrate is 600 bp long and has been blocked at one end with a biotin-streptavidin moiety to enforce unidirectional processing of the substrate (see ref. 1 for details).

1. Yeeles JT, van Aelst K, Dillingham MS, Moreno-Herrero F (2011) Recombination hotspots and single-stranded DNA binding proteins couple DNA translocation to DNA unwinding by the AddAB helicase-nuclease. *Mol Cell* 42(6):806–816.

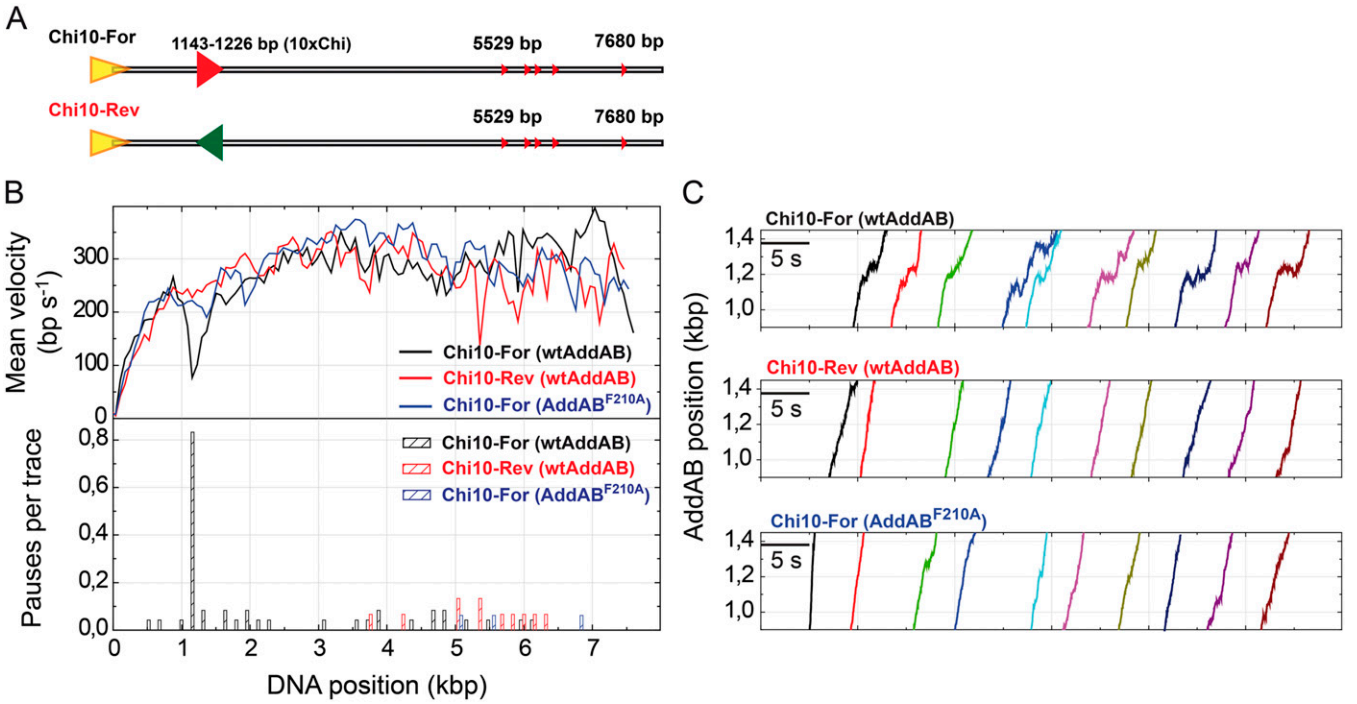

Fig. S3. The AddAB^{F210A} mutant does not pause at Chi. (*A*) DNA substrates containing 10 consecutive Chi sequences (10×Chi) either correctly oriented for AddAB recognition (Chi10-For) or in opposite orientation (Chi10-Rev). The 10×Chi locus is located ~1.1 kbp from the entry point. (*B*) Mean velocity graph and pause distribution histogram for wild-type AddAB and AddAB^{F210A} translocation on Chi10-For and Chi10-Rev substrates, showing wild-type AddAB-specific pausing at Chi. (*C*) Detail of pauses at the 10×Chi locus in Chi10-For and absence of pauses in Chi10-Rev substrates or when using AddAB^{F210A}.

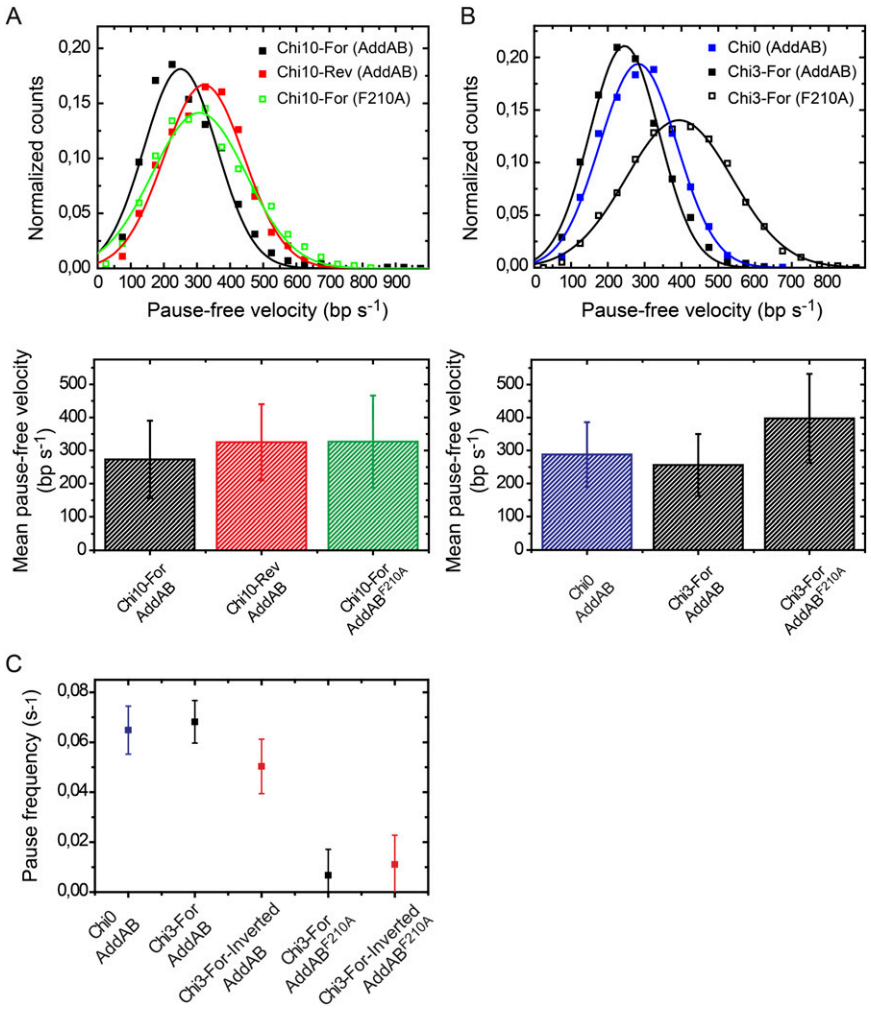

Fig. S4. The effect of Chi recognition on pause-free velocity distributions. (*A*) (*Upper*) Pause-free velocity distributions of WTAddAB and AddAB^{F210A} for substrates Chi10-For and Chi10-Rev. (*Lower*) Mean velocity values ± SEs. The presence of Chi sequences slows down the translocation rate of WTAddAB. (*B*) (*Upper*) Pause-free velocity distributions of WTAddAB and AddAB^{F210A} for substrates Chi0 and Chi3-For. (*Lower*) Mean velocity values ± SEs. Mutant AddAB^{F210A} translocated faster than the wild type but also presented larger velocity variability. (*C*) Pause frequency of AddAB and mutant AddAB^{F210A} for Chi0, Chi3-For, and Chi3-For-Inverted substrates as measured with our single-molecule assay. Use of a mutant with a significantly reduced ability to recognize Chi strongly decreased the frequency of all pausing on our DNA substrates.

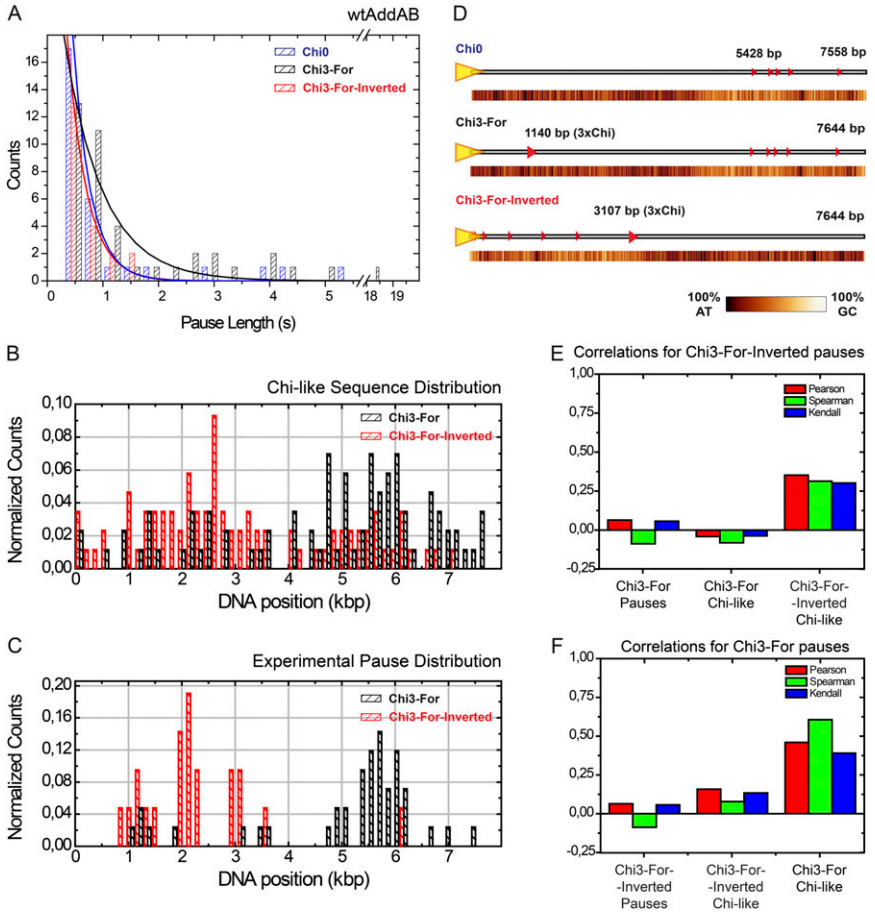

Fig. S5. Experimental pause length distribution and correlation between the location of pauses and Chi-like sequences. (*A*) AddAB pause length distribution for Chi0, Chi3-For, and Chi3-For-Inverted. Pauses were short and their duration followed an exponential distribution. (*B*) The Chi-like sequence distribution for the Chi3-For and Chi3-For-Inverted substrates. The number of Chi-like sequences in a particular bin (160 bp) was normalized by the total number of Chi-like sequences. (*C*) Experimental pause distribution of WTAddAB for Chi3-For and Chi3-For-Inverted substrates. Similarly, the number of pauses in each bin was divided by the total number of pauses. (*D*) GC-content distribution for the Chi0, Chi3-For, and Chi3-For-Inverted substrates. Color scale (from dark to bright) is 0–100% GC content in a running window of 16 bp. Note that a higher GC content region begins at ~4.5 kbp in Chi0, i.e., about 1,000 bp upstream of the position of the first Chi sequence. (*E*) Correlation between the experimental pause distribution for Chi3-For-Inverted and the location of Chi-like sequences. (*F*) Correlation between the experimental pause distribution for Chi3-For and the location of Chi-like sequences. The Pearson product moment correlation coefficient, the Spearman rank correlation coefficient, and the Kendall correlation coefficient were calculated using OriginLab.

Table S1. Summary of parameters of single-molecule magnetic tweezers experiments

Parameter	Chi0	Chi3-For	Chi3-For-Inverted	Chi10-For	Chi10-Rev	Chi10-For-For, first/second	Chi10-For-Rev, first/second	Chi10-Rev-For, first/second	Chi10-Rev-Rev, first/second
No. DNA molecules	20	24	22	24 16*	15	50	19	40 20*	20
No. pauses	31	42	22	46 3*	11	105	29	45 5*	21
No. pauses at 10×Chi	NA	NA	NA	20 0*	0	35/15	12/0	0/25 1/0*	0/1
N†	NA	NA	NA	5.2 ± 0.7	NA	3.9 ± 0.3/4.2 ± 0.4	NA	4.2 ± 0.4	NA
K†, s^{-1}	NA	NA	NA	3.5 ± 0.5	NA	2.1 ± 0.3/3.2 ± 0.3	NA	3.1 ± 0.3	NA

NA, not applicable.
*Using $AddAB^{F210A}$.
†Parameters of a normalized gamma function fitting of 10×Chi pause length distributions. Errors are SEs in the fit.

Table S2. Chi loci and oligonucleotide sequences

Oligo name	Oligonucleotide sequence, 5′→3′
3xChi locus	TAG CGG TAA ATG CAT AGC GGT ACG CGT ATA GCG GT
10×Chi locus	TCA GCG GCA GCG GA TAG CGG GAA GAG CGG ATT GAA GCG GCA AGA GCG GAA AGC GGA GCG CTT AGC GGG TCA GTA AAT GAA GCG GAA GCG GTT
FMH_F1_DIG	(Digoxigenin)GCCGCATAGTTAAGCCAGCCCCG
FMH_R1	CGAGCTCGGTACCCGGGGATCCG
FMH_F1	GCCGCATAGTTAAGCCAGCCCCG
FMH_R1_DIG	(Digoxigenin)CGAGCTCGGTACCCGGGGATCCG

Table S3. Oligonucleotides and templates for PCR substrate synthesis

Substrate	Oligonucleotides	Template
Chi0	FMH_F1_DIG/FMH_R1	pSP73-JY0-BbvCI
Chi3-For	FMH_F1_DIG/FMH_R1	pSP73-JY10-BbvCI
Chi3-For-Inverted	FMH_F1/FMH_R1_DIG	pSP73-JY10-BbvCI
Chi10-For	FMH_F1_DIG/FMH_R1	pSP73-JY0-BbvCI-Superchi
Chi10-Rev	FMH_F1_DIG/FMH_R1	pSP73-JY0-BbvCI-Reverse_Superchi
Chi10-For-For	FMH_F1_DIG/FMH_R1	pSP73-JY0-BbvCI-For-For
Chi10-For-Rev	FMH_F1_DIG/FMH_R1	pSP73-JY0-BbvCI-For-Rev
Chi10-Rev-For	FMH_F1_DIG/FMH_R1	pSP73-JY0-BbvCI-Rev-For
Chi10-Rev-Rev	FMH_F1_DIG/FMH_R1	pSP73-JY0-BbvCI-Rev-Rev

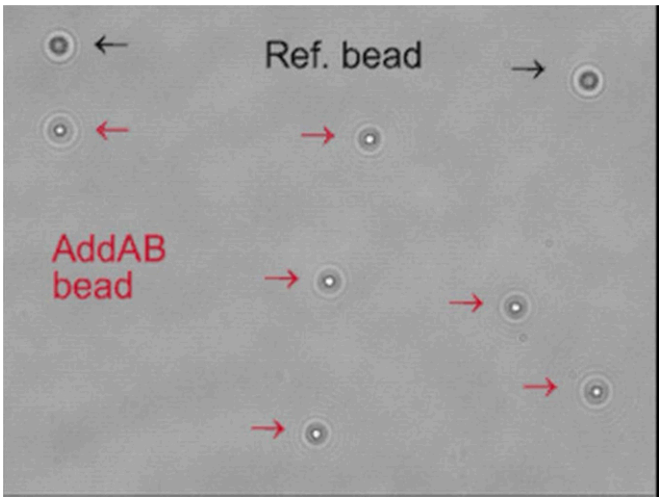

Movie S1. Real-time movie of AddAB translocation. Shown is an illustrative example of individual AddAB proteins translocating along DNA captured with video microscopy in a magnetic tweezers device. Initially, eight 1-μm beads appear in the field of view. Two of them are attached at a glass surface (Ref. Bead, black arrows) and six are connected to the glass surface through an individual AddAB–DNA interaction (AddAB bead, red arrows; see Fig. 1*B* for setup details). The difference in height between both AddAB and Ref. beads was readily distinguishable by their diffraction rings (Fig. 1*C*). Note that for the sake of clarity, in this example, the microscope was focused on the AddAB beads. Arrival of ATP (0:05 s) quickly triggered unidirectional translocation of AddAB along the DNA, dragging the AddAB beads toward the surface. Complete translocation lasts for about 12–20 s. Observe how beads translocate at slightly different velocities, highlighting the presence of static disorder. The beads stop at the surface and then, in some cases, we observe the loss of the bead (in the movie, at times 00:27, 00:42, and 00:45 s). There are at least three likely explanations for why the bead would be lost at this point: (*i*) A double-strand break is created by AddAB at the surface. AddAB has two nonsynchronized nuclease domains, each responsible for nicking of one of the two DNA strands. The nicking rate is low, and consequently nicks are far apart (hundreds to thousands of nucleotides) if the enzyme is moving fast. However, any blockage of translocation might greatly increase the chances of forming a DSB by making two nearby nicks on each strand of the duplex. AddAB could then dissociate by slipping off the DNA backward. (*ii*) Destabilization of the DIG–anti-DIG interaction that holds the DNA (and therefore the AddAB bead) to the surface could occur. (*iii*) In homologous recombination, AddAB must leave the DNA at some point to facilitate the subsequent step of strand invasion catalyzed by RecA. Some AddAB beads may simply dissociate from the DNA upon arrival to the end of the track. We note, however, that loss of beads was very rarely observed in the course of a translocation event. The total duration of the movie is 47 s and it was recorded at 120 frames per second.

Movie S1